Biochemical and Biophysical Research Communications 457 (2015) 378–384

Contents lists available at ScienceDirect

Biochemical and Biophysical Research Communications

journal homepage: www.elsevier.com/locate/ybbrc

Modeled microgravity suppressed invasion and migration of human glioblastoma U87 cells through downregulating store-operated calcium entry

Zi-xuan Shi [a, 1], Wei Rao [b, 1], Huan Wang [c], Nan-ding Wang [d], Jing-Wen Si [a], Jiao Zhao [a], Jun-chang Li [a, *], Zong-ren Wang [a, *]

[a] Department of Traditional Chinese Medicine, Xijing Hospital, Fourth Military Medical University, Xi'an, 710032, PR China
[b] Department of Neurosurgery, Xijing Hospital, Fourth Military Medical University, Xi'an, 710032, PR China
[c] Department of Dermatology, Tangdu Hospital, Fourth Military Medical University, Xi'an, 710032, PR China
[d] Department of Cardiology, Xi'an Traditional Chinese Medicine Hospital, Xi'an, 710032, PR China

ARTICLE INFO

Article history:
Received 19 December 2014
Available online 9 January 2015

Keywords:
Microgravity
Glioblastoma
Invasion
Migration
SOCE

ABSTRACT

Glioblastoma is the most common brain tumor and is characterized with robust invasion and migration potential resulting in poor prognosis. Previous investigations have demonstrated that modeled microgravity (MMG) could decline the cell proliferation and attenuate the metastasis potential in several cell lines. In this study, we studied the effects of MMG on the invasion and migration potentials of glioblastoma in human glioblastoma U87 cells. We found that MMG stimulation significantly attenuated the invasion and migration potentials, decreased thapsigargin (TG) induced store-operated calcium entry (SOCE) and downregulated the expression of Orai1 in U87 cells. Inhibition of SOCE by 2-APB or stromal interaction molecule 1 (STIM1) downregulation both mimicked the effects of MMG on the invasion and migration potentials in U87 cells. Furthermore, upregulation of Orai1 significantly weakened the effects of MMG on the invasion and migration potentials in U87 cells. Therefore, these findings indicated that MMG stimulation inhibited the invasion and migration potentials of U87 cells by downregulating the expression of Orai1 and sequentially decreasing the SOCE, suggesting that MMG might be a new potential therapeutic strategy in glioblastoma treatment in the future.

1. Introduction

Glioblastoma is the most common primary brain tumor in adults, which is characterized by uncontrolled cellular proliferation, extraordinary invasion and migration potentials and these features make this disease's treatment tough [1–3]. At present, though standard treatments of glioblastoma, including surgical resection, irradiation with adjuvant temozolomide and on recurrence, experimental chemotherapy, have gained improvements, the survival of patients remains poor and 2-year relative survival probability is low [2,3]. Inventing and improving novel therapeutic strategies are critically needed.

Recent years, magnetic fluid-modeled microgravity has been emerging as a new potential therapy for tumor treatment [4]. Considerable attentions were paid to the effects of microgravity on cellular behaviors, especially on tumor cells. Increasing investigations have indicated that microgravity has evident effects on the morphology, proliferation, apoptosis, invasion, migration, and even gene expression's variation [5,6]. Jing Li et al. found that microgravity insult would change the cytoskeleton and focal adhesions, and decrease migration in human breast carcinoma [7]. De Chang et al. found that microgravity treatment inhibited cell proliferation, migration, and invasion of human lung adenocarcinoma cell line [8]. Meanwhile, after microgravity insult, differentiation alteration and apoptosis increase have been found in human follicular thyroid carcinoma cells [9]. However, though a few studies have demonstrated that microgravity induced apoptosis in cultured glial cells [10], inhibited proliferation and enhanced chemical sensitivity of glioblastoma cells [11], the evident effects of

* Corresponding authors.
E-mail address: zongren@fmmu.edu.cn (Z.-r. Wang).
[1] These authors contributed equally to this work.

http://dx.doi.org/10.1016/j.bbrc.2014.12.120
0006-291X/

microgravity on glioblastoma cells have been poor investigated, especially on the invasion and migration potentials.

In this study, we applied a clinostat to model microgravity on the ground to investigate the effects of modeled microgravity (MMG) on the invasion and migration potentials of U87 cells. We found that MMG stimulation could attenuate the invasion and migration potentials by downregulating the expression of Orai1 and decreasing the SOCE, indicating that MMG might be a new good perspective in glioblastoma therapy and much more mechanism investigations should be paid to it.

2. Materials and methods

2.1. Cell culture

The human glioblastoma U87 cells were obtained from the Institute of Biochemistry and Cell Biology, SIBS, CAS. The cell line was cultured in complete Dulbecco's modified Eagle medium (DMEM) (Gibco, MD, USA), supplemented with 10% fetal bovine serum (Gibco, MD, USA), 100 U/ml penicillin and 0.1 mg/ml streptomycin (Gibco, MD, USA), in a humidified incubator with 5% CO_2 and 95% air.

2.2. Plasmids and transfections

The STIM1-shRNA (sc-76589-SH) and scramble-shRNA (Scr-shRNA) (sc-108060) were purchased from Santa Cruz Biotech (Santa Cruz, CA, USA). Full-length cDNAs for Orai1 (BC015369) was synthesized and subcloned into pcDNA3.1 vector. U87 cells were transfected with plasmids using Lipofectamine 2000 transfection reagent according to the manufacturer's protocol (Invitrogen, CA, USA). Optimal transfection conditions were determined by using GFP-labeled nonspecific shRNA. Protein expression levels were detected to evaluate the efficiency of downregulation or upregulation 72 h after transfection.

2.3. Clinostat to model microgravity (MMG)

A 2D-clinostat device from the Fourth Military Medical University was applied in this study [12]. Cells were initially seeded on coverslips which were 2.55 × 2.15 cm^2. After the cells adhering to the coverslips for 6 h, the coverslips were inserted into the fixtures of chambers, and then the chambers were filled completely with DMEM with 10% FBS without any air bubbles existing to avoid the cell surface shearing. Finally, these chambers underwent rotation at 30 rpm around the vertical axis for 24, 48 or 72 h respectively. Normal gravity (NG) group was static control culture which was kept in the same clinostat conditions without rotation. The average gravitational force acting on the cells generated by the 2D-clinostat is reduced to about 10^{-3} G, compared with the NG, namely 1 G. After treatments, the cells were applied in the follow experiments.

2.4. Wound healing assay

The wound healing assay was carried out to evaluate the migration potential of the U87 cells. Cells were initially seeded on coverslips at a density of 5×10^4/well. After the cells adhering to the coverslips for 6 h, a line was scratched with a sterile 200 μl pipette tip across the coverslips and the coverslips were inverted into the chamber. Then, both NG and MMG groups were obtained corresponding treatments as described above. The wounded areas were photographed at the predicted times by inverted phase contrast microscope (Olympus, Tokyo, Japan). The wound healing effect was calculated by the equation ((the wound healing area/the cell-free area of the initial scratch) × 100%).

2.5. Transwell invasion assay

Transwell invasion assay was conducted with Transwell chamber (24-well insert; pore size, 8 μm; Merck Millipore, Darmstadt, Germany). Matrigel Matrix (BD Biosciences, CA, USA) was diluted with DMEM at the ratio of 1:8 on ice, and 100 μl mixture was added into each chamber. Then, the chambers were kept at 37 °C overnight. On the second day, 750 μl DMEM containing 10% FBS was added to the bottom of the chambers in the well and 200 μl cell suspension at the density of 1×10^5/ml was seeded into the top chamber. After a culture of 24 h, the non-invading cells on the top chamber were removed with cotton swab. Then the chambers were washed twice with PBS, fixed with 75% alcohol for 10 min, stained with 0.5% Crystal Violet for 5 min at room temperature (RT) and photographed in four independent ×10 fields/well. The stained cells were counted to quantify the invasive cells.

2.6. Calcium imaging

Briefly, U87 cells grown on coverslips were loaded with Fura-2AM (5 μM) (Molecular Probes, OR, USA) in Hanks Balanced Salt Solution supplemented with 20 mM D-glucose and 10 mM HEPES (HBSS) (Gibco, MD, USA) for 45 min, and equilibrated for 30 min in dark at RT. Then, cells were tightly mounted on open-bath imaging chamber containing HBSS. Using the Nikon inverted fluorescence microscope, cells were excited at 345 and 385 nm and the emission fluorescence at 510 nm was recorded in an XYT-plane fashion. Images were collected and analyzed with the MetaFluor image-processing software (Universal Imaging Corp, PA, USA). Standard "Ca^{2+}-off and Ca^{2+}-on" protocol was used to detect the SOCE. After the baseline recording for 120 s in Ca^{2+}-free HBSS, the recording buffer was changed with Ca^{2+}-free HBSS supplemented with TG (2 μM) and the calcium signaling was recorded for 720 s. Then, the buffer was changed with HBSS supplemented with TG (2 μM) and the calcium signaling was recorded for 360 s. The results were calculated and shown as F/F_0 and area under curve (AUC).

2.7. Western blot

Protein was extracted from U87 cells with RIPA lysis buffer. Protein concentration was quantified by using a BCA protein kit (Thermo Scientific, USA). 30 μg protein was loaded on 10% SDS-PAGE gels. After electrophoresis, the proteins were transferred to nitrocellulose membranes. Then the membranes were blocked with 5% skim milk and incubated at 4 °C overnight with the appropriate primary antibodies: STIM1 (1:1000) (CST, Danvers, MA, USA), Orai1 (1:500) (Santa Cruz Biotech, Santa Cruz, CA, USA) and β-Actin (1:2000) (Abcam, MA, USA). Immunoreactivity was detected by incubation with horseradish peroxidase-conjugated secondary antibodies (1:20000, CST, MA, USA) followed by chemiluminescent substrate development (Thermo Scientific, USA). Optical densities of the bands were calculated using a MiVnt image analysis system (Bio-Rad, CA, USA).

2.8. Quantitative RT-PCR (qRT-PCR)

A 2 μg template RNA was used to synthesize the first strand of cDNA using a reverse transcription kit (Takara, Dalian, China). Real-time PCR of cDNA was performed using the forward and reverse primer sequences: STIM1: forward: 5′-AGG AGC CTC ATC CTA ATC TCA CTC A-3′; reverse: 5′-GGC ATC CAC TCA TGC TCC AA-3′; STIM2:

forward: 5′-ATG TCA CTG AGT CCA CCA TGC TTT A-3′; reverse: 5′-TCT CTG TGC AGA TGG CTG TGT TTA-3′; Orai1: forward: 5′-CTT CGC CGT CCA CTT CTA CC-3′; reverse: 5′-CTG TAA GCG GGC AAA CTC C-3′; Orai2: forward: 5′-GGG TCT TCG TGT CAC AGC TTC A-3′; reverse: 5′-GCA CTC CTG CAG AGC ACA CTT TAG-3′; GAPDH: forward: 5′-TGG TGA AGA CGC CAG TGG A-3′; reverse: 5′-GCA CCG TCA AGG CTG AGA AC-3′. Samples were tested in triplicates and data from four independent experiments were used for analysis. Relative gene expression was calculated using the $2^{-\Delta\Delta CT}$ method [13].

2.9. Statistical analysis

All of the experiments were performed at least four times. The values were expressed in mean ± SEM, and analyzed by ANOVA followed by Bonferroni's multiple comparisons or unpaired t-test with SPSS 22.0 statistical software (IBM, Armonk, New York, USA). A value of $p < 0.05$ was considered to be statistically significant.

3. Results

3.1. MMG inhibited the invasion and migration potentials in U87 cells

To investigate whether MMG stimulation had effects on the invasion and migration potentials of U87 cells, the Transwell invasion and wound healing assay were applied. As shown in Fig. 1A and B, the cell-free wound area of the U87 cells monolayers stimulated by MMG for 48 and 72 h converged significantly more slowly compared with NG group. However, no significant difference was observed in 24 h subgroup. Furthermore, Transwell invasion assay indicated that MMG stimulation, no matter 24, 48 or 72 h, significantly attenuated the invasion potential compared with NG group (Fig. 1C and D). We could conclude that MMG stimulation would alleviate the U87 cells invasion and migration potentials and might the more time handled, the less potential the U87 cells had. Because MMG treatment for 72 h induced approximate 50% decrease of the invasion and migration potentials, this timepoint was used in the following experiments.

3.2. MMG decreased TG-induced SOCE and downregulated the expression of Orai1

After confirmed the role of MMG in the invasion and migration potentials, we further studied whether MMG had effects on SOCE, which played crucial roles in regulating the calcium hemostat in non-excited cell and regulating the cell migration. As shown in Fig. 2A and B, MMG stimulation for 72 h significantly decreased the TG-induced SOCE to 41% of that of NG group, but there was no difference in TG-induced release of calcium store. Then, to clarify the reason of decreasing SOCE, the expression changes of STIM1, STIM2, Orai1 and Orai2, which were important compositions of SOCE, were detected by qRT-PCR, finding that the expression of Orai1 but not STIM1, STIM2 and Orai2 was significantly downregulated to 48.7% of that of NG group (Fig. 2C). Furthermore, Western blot also verified that the protein level of Orai1 was downregulated (Fig. 2D). Therefore, MMG might downregulate the SOCE of U87 cells by decreasing the expression of Orai1.

3.3. Inhibition of SOCE mimicked the effects of MMG on the invasion and migration potentials in U87 cells

After observed the decreases in the invasion and migration potentials and SOCE in MMG-treated U87 cells, we further explicated whether inhibition of SOCE mimicked the role of MMG in the invasion and migration potentials in U87 cells by using pharmacological inhibitor 2-APB and STIM1 RNA interfere (RNAi). As verified by western blot, the expression of STIM1 was successfully downregulated to 23.4% compared with Scr-shRNA group (Fig. 3A). After tranfected with shRNA for 72 h, the U87 cells were used to calcium imaging. We found that STIM1 RNAi significantly inhibited the TG-induced SOCE but had no effects on the TG-induced release

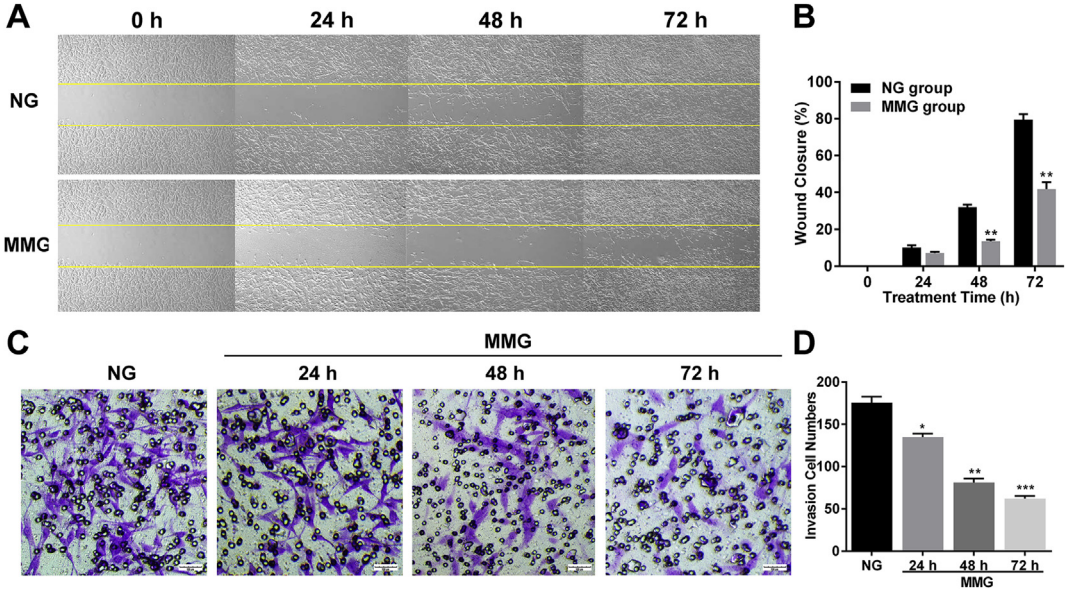

Fig. 1. MMG inhibited the invasion and migration potentials in U87 cells. The cell migration potential was assessed by wound healing assay. The images were acquired immediately 24, 48 or 72 h after scratching. The yellow solid lines indicated the original scratching zone (A). The wound healing effect was calculated by the equation ((the wound healing area/the cell-free area of the initial scratch) × 100%) (B). Transwell invasion assay indicated the decreasing invasive potential of the MMG treatment as compared with that of NG condition (C and D). Data were represented as means ± SEM from four experiments. Scale bars = 100 μm $^{*}p < 0.05$, $^{**}p < 0.01$, $^{***}p < 0.001$ vs. NG group. (For interpretation of the references to color in this figure legend, the reader is referred to the web version of this article.)

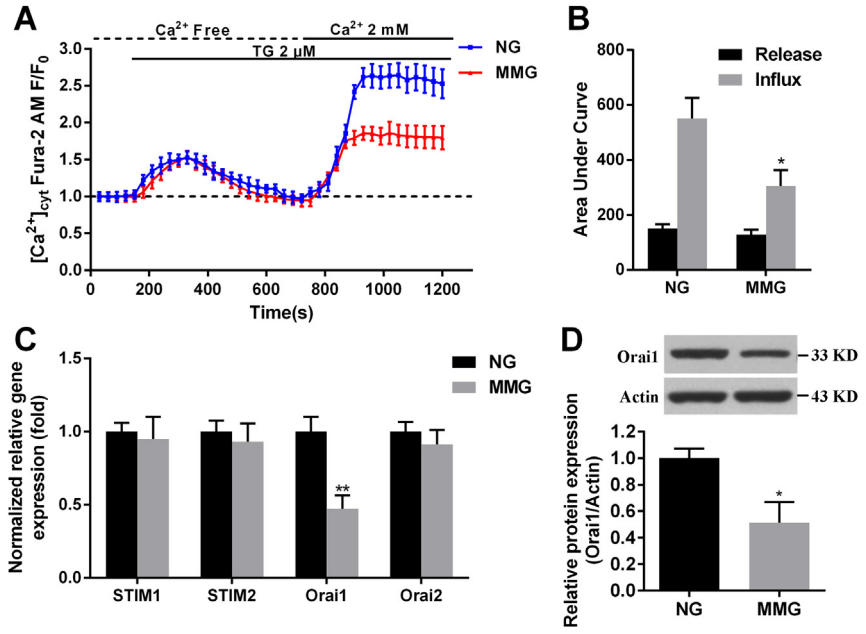

Fig. 2. MMG decreased SOCE and downregulated the expression of Orai1. After cultured under NG or MMG condition for 72 h, U87 cells grown on the coverslips were subjected to calcium imaging. "Ca^{2+}-off/Ca^{2+}-on" protocol was employed using TG to measure SOCE (A). The AUC was calculated and shown as a bar graph (B). After cultured under NG or MMG condition for 72 h, the U87 cells were harvested and used to qRT-PCR for detecting STIM1, STIM2, Orai1 and Orai2 (C) and to western blot for detecting Orai1 (D). Data were represented as means ± SEM from four experiments. $^{*}p < 0.05$, $^{**}p < 0.01$ vs. NG group.

of calcium store (Fig. 3B and C), compared with normal or Scr-shRNA group. Similarly, compared with normal group, application of 2-APB (75 μM, DMSO 0.5‰) also significantly inhibited SOCE (Fig. 3B and C). Furthermore, application of STIM1 RNAi or 2-APB both significantly alleviated the invasion and migration potential in U87 cells by Transwell invasion (Fig. 3D) and wound healing (Fig. 3E) assay. Therefore, inhibition of SOCE mimicked the effects of MMG on the invasion and migration potentials in U87 cells.

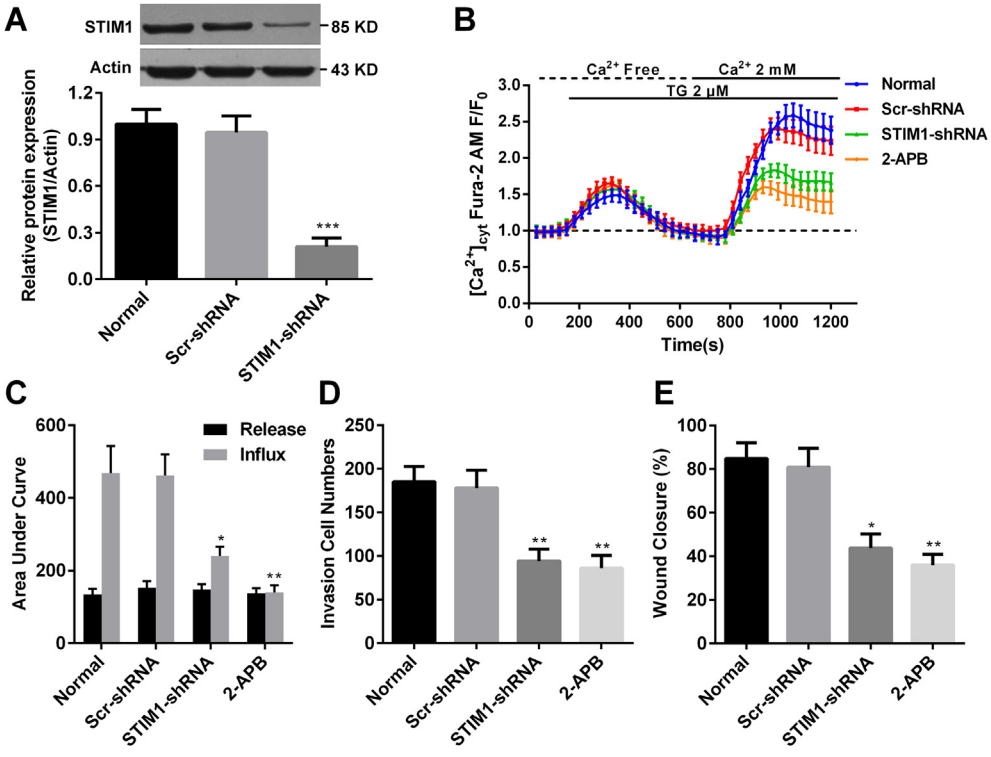

Fig. 3. Inhibition of SOCE mimicked the effects of MMG on the invasion and migration potentials in U87 cells. U87 cells were transfected with Scr-shRNA or STIM1-shRNA for 72 h, and the expression of STIM1 was examined by Western Blot analysis (A). After U87 cells were pretreated with 2-APB (75 μM) for 20 min or transfected with shRNA for 72 h, the SOCE was detected by calcium imaging according to "Ca^{2+}-off/Ca^{2+}-on" protocol (B). The AUC was calculated and shown as a bar graph (C). The cell invasion potential was evaluated by Transwell analysis. The invasion numbers were counted and shown as bar graph (D). The wound healing assay was used to evaluate the migration potential (E). Data were represented as means ± SEM from four experiments. $^{*}p < 0.05$, $^{**}p < 0.01$, $^{***}p < 0.001$ vs. Normal group.

3.4. Upregulation of Orai1 restored the decreasing invasion and migration potentials in U87 cells induced by MMG

To further clarify the roles of SOCE in MMG induced decreasing invasion and migration potentials, we upregulated the expression of Orai1 to study whether MMG affected the invasion and migration potentials by downregulating Orai1. After transfected with pcDNA3.1-Orai1 for 48 h (Orai1 O/E) and then subjected to MMG for 72 h, the U87 cells were harvested for western blot detection, showing that transfection of pcDNA3.1-Orai1 successfully eliminated MMG-induced downregulation of Orai1 and significantly increased the expression of Orai1 by 1.87 fold of that of normal group (Fig. 4A). Besides, calcium imaging also found that upregulation of Orai1 successfully rescued the decreasing SOCE caused by MMG and slightly exceeded the SOCE of that of normal group (Fig. 4B and C). Further, compared with control or pcDNA3.1 vector group, the invasion (Fig. 4D) and migration (Fig. 4E) potentials in U87 cells were significantly increased in Orai1 O/E group and there was no significant difference between pcDNA3.1-Orai1 and normal group, indicating that MMG might decrease the invasion and migration potentials in U87 cells by downregulating the expression of Orai1, and sequentially inhibiting the SOCE.

4. Discussion

Increasing studies have demonstrated that MMG had evident effects on the cellular proliferation, apoptosis, invasion and migration, and gene expression, especially in tumor cells [5,6,14]. Extraordinary invasion and migration potentials were the hallmarks of glioblastoma cell. However, it is not clear that whether MMG had effects on the invasion and migration potentials in glioblastoma. In this study, we found that the invasion and migration potentials of U87 cells were sensitive to MMG stimulation. After exposed to MMG for 24, 48 or 72 h, U87 cells invaded and migrated more slowly than NG group, and it was in time-dependence to some degree, indicating MMG might inhibit the invasion and migration potentials of U87 cells. These results were in consistent with previous studies in other tumor cells, such as melanomas [15], human breast cancer [16] and follicular thyroid carcinoma cells [9]. Jing Li et al. found that microgravity had closely associated with changing focal adhesion and cytoskeleton, and decreasing migration potential in human breast carcinoma [7]. De Chang et al. also found that microgravity inhibited migration and invasion of human lung adenocarcinoma cell line [8]. Thus, MMG might have distinct effects on inhibiting the invasion and migration potentials in glioma cells.

Ca^{2+}, as a ubiquitous second messenger, is crucially involved in the regulation of cell invasion and migration [17]. Intracellular Ca^{2+} had important roles in turnover of focal adhesion and arrangement of cytoskeletal protein, which determined how efficiently a cell invaded and migrated by regulating FAK [18], calcineurin [19] or S100A4 [20]. Many calcium channels, including store-operated calcium channels (SOCs), IP3R and RYR, regulated invasion and migration in several cancer cell lines [18,21,22]. Specially, SOCE, which was mainly mediated by STIM1 and SOCs (Orai1, Orai2), had

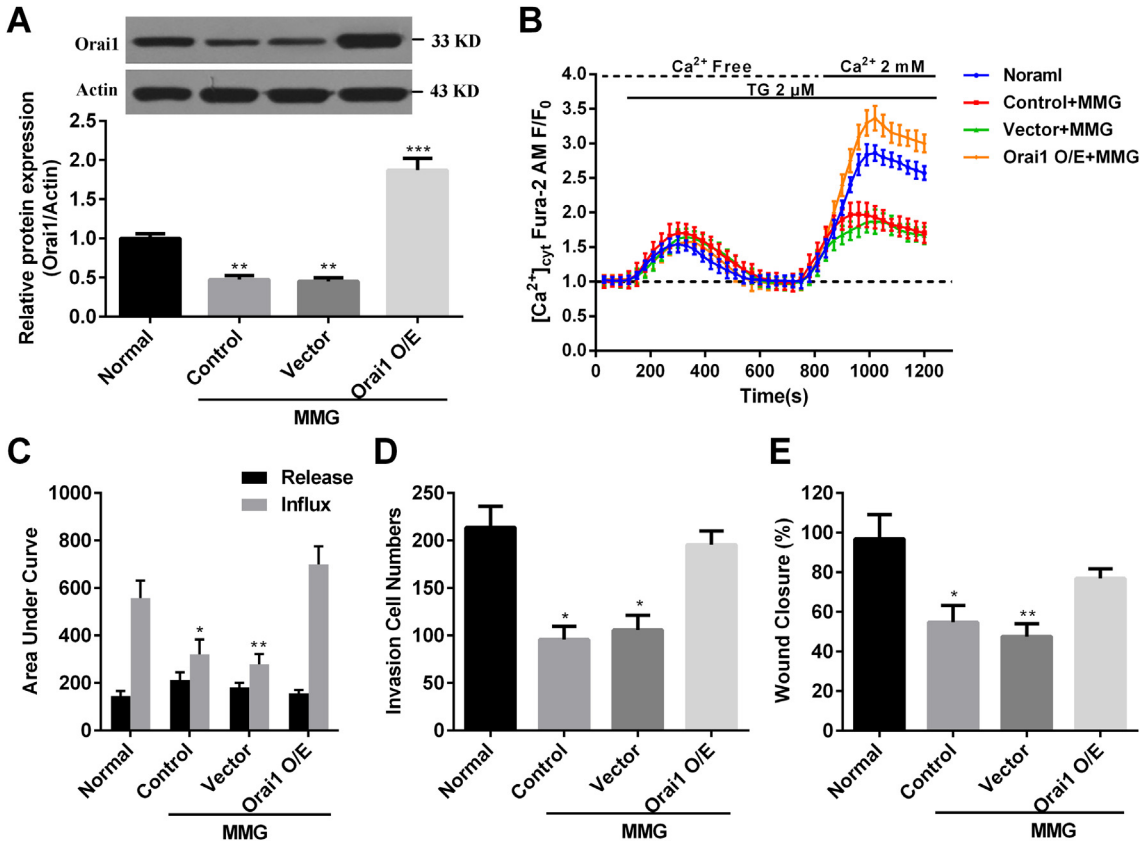

Fig. 4. Upregulation of Orai1 restored the decreasing invasion and migration potentials induced by MMG in U87 cells. After transfected with vector or pcDNA3.1-Orai1 for 48 h (Orai1 O/E) and then subjected to MMG for 72 h, the U87 cells were harvested and used to western blot for detecting the expression of Orai1 (A). After U87 cells were successfully overexpressed of Orai1 and cultured under MMG condition for 72 h, the SOCE was detected by calcium imaging according to "Ca^{2+}-off/Ca^{2+}-on" protocol (B). The AUC was calculated and shown as a bar graph (C). The cell invasion potential was evaluated by Transwell analysis. The invasion numbers were counted and shown as bar graph (D). The wound healing assay was used to evaluate the migration potential (E). Data were represented as means ± SEM from four experiments. $^{*}p < 0.05$, $^{**}p < 0.01$, $^{***}p < 0.001$ vs. Normal group.

a tight relationship with Ca^{2+} homeostasis by sensing endoplasmic reticulum Ca^{2+} level and mediating extracellular Ca^{2+} entry [23]. SOCE has intimately linked to invasion and migration in several tumor cell lines by affecting the focal adhesion turnover [21,24]. Moreover, abundant investigations had also indicated that microgravity affected the intracellular Ca^{2+} signaling [25–27]. Then, whether MMG had some effects on SOCE? Our studies found the expression of Orai1, which was the predominant SOCs expressed in non-excited cells, not STIM1, STIM2 and Orai2, was downregulated after MMG treatment for 72 h. Furthermore, the TG-induced decreasing SOCE was in parallel with the reduction of the invasion and migration potentials in U87 cells. Therefore, we speculated that MMG might downregulated the expression of Orai1, sequentially inhibited the SOCE and then weakened the invasion and migration potentials of U87 cells.

In further study, we firstly validated the effects of SOCE inhibition on the invasion and migration potentials of U87 cells. Application of 2-APB, an intensively-used SOCE inhibitor, inhibited the TG-induced SOCE and the invasion and migration potentials of U87 cells. Downregulation of STIM1, the crucial regulator of SOCE, had consistent results with 2-APB application. These results were in agree with previous studies which indicated that SOCE regulated migration and invasion of human breast cancer cell [21], hepatocarcinoma cell [28], glioblastoma cell [24,29]. Furthermore, we successfully upregulated the expression of Oria1 to observe whether Orai1 upregulation rescued MMG induced decreasing invasion and migration potentials in U87 cells. Calcium imaging showed that upregulation of Orai1 restored the decreasing SOCE induced by MMG. Although the expression of Orai1 in Orai1 O/E group was approximately 2 folds of that of normal group, there was no significant difference of SOCE between Orai1 O/E and normal group. This phenomena might due to that appropriate STIM1/Orai1 ratio was key point in regulating SOCE. In response to the increasing SOCE, upregulation of Orai1 diminished the effects of MMG on the invasion and migration potentials of U87 cells. Thus, the results above showed that MMG inhibited the invasion and migration potentials of U87 cells through downregulating the expression of Orai1 and then decreasing of SOCE.

In summary, our study investigated the relationships between MMG and the invasion and migration potentials in human glioblastoma U87 cells, demonstrating that MMG inhibited the migration and invasion potentials. This effects might partially due to that MMG downregulated the expression of Orai1 and then decreased the SOCE. Thus, our findings suggest that MMG would be a new potential glioma therapeutic strategy in the future. Obviously, further study about the exact regulating mechanisms of MMG on Orai1 and corresponding studies in vivo are warranted.

Conflict of interest

The authors have no conflicts of interest to declare.

Acknowledgment

The authors give thanks to the Neurosurgery department, Xijing Hospital, Fourth Military Medical University for the technical assistances. This project is supported by the National Natural Science Foundation of China (81273879).

Transparency document

The transparency document associated with this article can be found in the online version at http://dx.doi.org/10.1016/j.bbrc.2014.12.120.

References

[1] H. Ohgaki, P. Kleihues, Epidemiology and etiology of gliomas, Acta Neuropathol. 109 (2005) 93–108.
[2] J.A. Schwartzbaum, J.L. Fisher, K.D. Aldape, M. Wrensch, Epidemiology and molecular pathology of glioma, Nat. Clin. Pract. Neurol. 2 (2006) 494–503 quiz 491 p following 516.
[3] F.H. Hochberg, N.A. Atai, D. Gonda, M.S. Hughes, B. Mawejje, L. Balaj, R.S. Carter, Glioma diagnostics and biomarkers: an ongoing challenge in the field of medicine and science, Expert Rev. Mol. Diagn. 14 (2014) 439–452.
[4] J. Chen, Z. Yan, R. Liu, N. Wang, J. Li, Z. Wang, Magnetic fluid-modeled microgravity: a novel way to treat tumor, Med. Hypotheses 77 (2011) 953–955.
[5] J. Vassy, S. Portet, M. Beil, G. Millot, F. Fauvel-Lafeve, G. Gasset, D. Schoevaert, Weightlessness acts on human breast cancer cell line MCF-7, Adv. Space Res. 32 (2003) 1595–1603.
[6] L.S. Mangala, Y. Zhang, Z. He, K. Emami, G.T. Ramesh, M. Story, L.H. Rohde, H. Wu, Effects of simulated microgravity on expression profile of microRNA in human lymphoblastoid cells, J. Biol. Chem. 286 (2011) 32483–32490.
[7] J. Li, S. Zhang, J. Chen, T. Du, Y. Wang, Z. Wang, Modeled microgravity causes changes in the cytoskeleton and focal adhesions, and decreases in migration in malignant human MCF-7 cells, Protoplasma 238 (2009) 23–33.
[8] D. Chang, H. Xu, Y. Guo, X. Jiang, Y. Liu, K. Li, C. Pan, M. Yuan, J. Wang, T. Li, C. Liu, Simulated microgravity alters the metastatic potential of a human lung adenocarcinoma cell line, Vitro Cell. Dev. Biol. Anim. 49 (2013) 170–177.
[9] D. Grimm, J. Bauer, P. Kossmehl, M. Shakibaei, J. Schoberger, H. Pickenhahn, G. Schulze-Tanzil, R. Vetter, C. Eilles, M. Paul, A. Cogoli, Simulated microgravity alters differentiation and increases apoptosis in human follicular thyroid carcinoma cells, FASEB J 16 (2002) 604–606.
[10] B.M. Uva, M.A. Masini, M. Sturla, F. Bruzzone, M. Giuliani, G. Tagliafierro, F. Strollo, Microgravity-induced apoptosis in cultured glial cells, Eur. J. Histochem. 46 (2002) 209–214.
[11] M. Takeda, T. Magaki, T. Okazaki, Y. Kawahara, T. Manabe, L. Yuge, K. Kurisu, Effects of simulated microgravity on proliferation and chemosensitivity in malignant glioma cells, Neurosci. Lett. 463 (2009) 54–59.
[12] F. Shi, Y.C. Wang, T.Z. Zhao, S. Zhang, T.Y. Du, C.B. Yang, Y.H. Li, X.Q. Sun, Effects of simulated microgravity on human umbilical vein endothelial cell angiogenesis and role of the PI3K-Akt-eNOS signal pathway, PLoS One 7 (2012) e40365.
[13] K.J. Livak, T.D. Schmittgen, Analysis of relative gene expression data using real-time quantitative PCR and the 2(−Delta Delta C(T)) method, Methods 25 (2001) 402–408.
[14] C.Y. Kang, L. Zou, M. Yuan, Y. Wang, T.Z. Li, Y. Zhang, J.F. Wang, Y. Li, X.W. Deng, C.T. Liu, Impact of simulated microgravity on microvascular endothelial cell apoptosis, Eur. J. Appl. Physiol. 111 (2011) 2131–2138.
[15] K. Ivanova, P. Eiermann, W. Tsiockas, J. Hauslage, R. Hemmersbach, R. Gerzer, Natriuretic peptide-sensitive guanylyl cyclase expression is down-regulated in human melanoma cells at simulated weightlessness, Acta Astronaut. 68 (2011) 652–655.
[16] A. Qian, W. Zhang, L. Xie, Y. Weng, P. Yang, Z. Wang, L. Hu, H. Xu, Z. Tian, P. Shang, Simulated weightlessness alters biological characteristics of human breast cancer cell line MCF-7, Acta Astronaut. 63 (2008) 947–958.
[17] P. Pomorski, Calcium regulation of cell migration, Postepy Biochem. 55 (2009) 163–170.
[18] R.S. Fan, R.O. Jacamo, X. Jiang, J. Sinnett-Smith, E. Rozengurt, G protein-coupled receptor activation rapidly stimulates focal adhesion kinase phosphorylation at Ser-843. Mediation by Ca^{2+}, calmodulin, and Ca^{2+}/calmodulin-dependent kinase II, J. Biol. Chem. 280 (2005) 24212–24220.
[19] S. Lev, H. Moreno, R. Martinez, P. Canoll, E. Peles, J.M. Musacchio, G.D. Plowman, B. Rudy, J. Schlessinger, Protein tyrosine kinase PYK2 involved in Ca(2+)-induced regulation of ion channel and MAP kinase functions, Nature 376 (1995) 737–745.
[20] K. Boye, G.M. Maelandsmo, S100A4 and metastasis: a small actor playing many roles, Am. J. Pathol. 176 (2010) 528–535.
[21] S. Yang, J.J. Zhang, X.Y. Huang, Orai1 and STIM1 are critical for breast tumor cell migration and metastasis, Cancer Cell. 15 (2009) 124–134.
[22] J.P. Chen, Y. Luan, C.X. You, X.H. Chen, R.C. Luo, R. Li, TRPM7 regulates the migration of human nasopharyngeal carcinoma cell by mediating Ca(2+) influx, Cell. Calcium 47 (2010) 425–432.
[23] J. Soboloff, B.S. Rothberg, M. Madesh, D.L. Gill, STIM proteins: dynamic calcium signal transducers, Nat. Rev. Mol. Cell. Biol. 13 (2012) 549–565.
[24] M. Zhu, L. Chen, P. Zhao, H. Zhou, C. Zhang, S. Yu, Y. Lin, X. Yang, Store-operated Ca^{2+} entry regulates glioma cell migration and invasion via modulation of Pyk2 phosphorylation, J. Exp. Clin. Cancer Res. 33 (2014) 98.
[25] M.Z. Luo, Z.Q. Yang, J.B. Li, H.Y. Xu, S.S. Li, W. Zhang, A.R. Qian, P. Shang, Calcium influx through stretch-activated channels mediates microfilament reorganization in osteoblasts under simulated weightlessness, Adv. Space Res. 51 (2013) 2058–2068.
[26] T.B. Damm, S. Richard, S. Tanner, F. Wyss, M. Egli, A. Franco-Obregon, Calcium-dependent deceleration of the cell cycle in muscle cells by simulated microgravity, Faseb J. 27 (2013) 2045–2054.
[27] M.-J. Xie, L.-F. Zhang, J. Ma, H.-W. Cheng, Functional alterations in cerebrovascular K(+) and Ca(2+) channels are comparable between simulated

microgravity rat and SHR, American journal of physiology, Heart Circ. Physiol. 289 (2005) H1265–H1276.

[28] N. Yang, Y. Tang, F. Wang, H.B. Zhang, D. Xu, Y.F. Shen, S.H. Sun, G.S. Yang, Blockade of store-operated Ca^{2+} entry inhibits hepatocarcinoma cell migration and invasion by regulating focal adhesion turnover, Cancer Lett. 330 (2013) 163–169.

[29] R.K. Motiani, M.C. Hyzinski-Garcia, X.X. Zhang, M.M. Henkel, I.F. Abdullaev, Y.H. Kuo, K. Matrougui, A.A. Mongin, M. Trebak, STIM1 and Orai1 mediate CRAC channel activity and are essential for human glioblastoma invasion, Pflugers Archiv. European J. Physiol. 465 (2013) 1249–1260.